Magnetized (2 + 1)-dimensional Gross-Neveu model at finite density

Julian J. Lenz,[1,2,*] Michael Mandl,[1,†] and Andreas Wipf[1,‡]

[1]*Theoretisch-Physikalisches Institut, Friedrich-Schiller-Universität Jena, D-07743 Jena, Germany*
[2]*Swansea Academy of Advanced Computing, Swansea University, Fabian Way, SA1 8EN, Swansea, Wales, United Kingdom*

(Received 2 August 2023; accepted 2 September 2023; published 11 October 2023)

We perform a lattice study of the $(2+1)$-dimensional Gross-Neveu model in a background magnetic field B and at nonzero chemical potential μ. The complex-action problem arising in our simulations using overlap fermions is under control. For $B=0$, we observe a first-order phase transition in μ even at nonvanishing temperatures. Our main finding, however, is that the rich phase structure found in the limit of infinite flavor number N_{f} is washed out by the fluctuations present at $N_{\mathrm{f}}=1$. We find no evidence for inverse magnetic catalysis, i.e., the decrease of the order parameter of chiral symmetry breaking with B for μ close to the chiral phase transition. Instead, the magnetic field tends to enhance the breakdown of chiral symmetry for all values of μ below the transition. Moreover, we find no trace of spatial inhomogeneities in the order parameter. We briefly comment on the potential relevance of our results for QCD.

DOI: 10.1103/PhysRevD.108.074508

I. INTRODUCTION

The study of quantum chromodynamics (QCD) at finite baryon density is a highly nontrivial endeavor due to the complex-action problem, which prevents the use of lattice simulations based on importance sampling [1], the most reliable *ab initio* tool for the nonperturbative study of strongly interacting matter. With lattice QCD no longer at one's disposal in a parameter regime that is, e.g., relevant for the physics of compact stellar objects like neutron stars, an alternative is much needed. While considerable effort is put into finding methods that circumvent the complex-action problem, another approach entirely is the study of low-energy effective theories, which reproduce QCD phenomenology within their range of validity.

Prominent examples of such effective field theories are those based on chiral perturbation theory [2] and the four-Fermi theories (4FTs). The latter arise in the low-energy limit of QCD [3] and are capable of capturing a number of essential features of QCD, in particular, chiral symmetry and its spontaneous breakdown. There are examples of 4FTs that are amenable to lattice studies at finite density, since they do not suffer from a complex-action problem due to their rather simple structure—see, e.g., [4]. In fact, a great part of our current understanding of finite-density QCD stems from the investigation of 4FTs [5–7].

One particularly interesting question is how the structure of strongly interacting matter changes under the influence of background magnetic fields [8–10]. This is due to the fact that magnetic fields of the order of the QCD scale are generated in noncentral heavy-ion collisions [11], are present in the cores of magnetars [12], and were likely produced during the electroweak phase transition [13]. However, because of the aforementioned limitations of lattice simulations, magnetized systems at finite baryon density are still quite elusive.

To this end, we perform in this work a lattice study of the Gross-Neveu (GN) model [14], the simplest 4FT, in $(2+1)$ space-time dimensions. Extending our previous work [15], which was concerned with the magnetized GN model at zero density but finite temperature, we here work at low temperature but nonzero chemical potential. In [15], it became clear that this simple model fails to correctly describe the phenomenology of magnetized QCD [16,17] both in and beyond the mean-field limit. However, we also emphasized its role as a starting point for the description of QCD in background magnetic fields by means of beyond-mean-field effective models.

It shall be one of our goals to shed light on the question of how much of the rich phase structure the model exhibits in the mean-field limit [18] persists when quantum fluctuations are taken into account. Work in this direction has already been done using the optimized perturbation theory (OPT) technique [19], but, to the best of our knowledge, there exist no *ab initio* lattice simulations in the literature

*j.j.lenz@swansea.ac.uk
†michael.mandl@uni-jena.de
‡wipf@tpi.uni-jena.de

that are concerned with that question. Furthermore, we investigate whether the magnetic field induces spatial inhomogeneities at finite density as it likely does at very strong fields in $3+1$ dimensions [20–23]. Lastly, as a long-term goal, we aim at understanding properly to what extent our findings are of relevance for QCD.

We provide access to our simulation data online [24] in order to ensure the reproducibility of our results in accordance with the FAIR[1] guiding principles [26]. Moreover, our data analysis scripts can be found in [27].

The outline of this work is as follows. In Sec. II, we introduce the GN model and discuss how chiral symmetry and its spontaneous breakdown are affected by a chemical potential and an external magnetic field in the mean-field limit. In particular, we discuss the complicated phase structure arising due to fermionic Landau levels. Section III outlines our lattice formalism using overlap fermions, putting a particular emphasis on the complex-action problem present in our simulations and how it is avoided. We then present our simulation results obtained at finite density and magnetic field in Sec. IV before discussing their relevance in Sec. V. A large part of our formalism and notation was introduced in [15], and we shall refer to that work on various occasions for brevity.

II. ANALYTICAL RESULTS

The GN model at finite density (determined by the chemical potential μ) and magnetic field (described by the vector potential A_μ) in the chiral limit is defined by the Lagrangian

$$\mathcal{L}_\sigma = \mathrm{i}\bar{\psi}(\partial\!\!\!/ + \mathrm{i}eA\!\!\!/ + \sigma + \mu\gamma_0)\psi + \frac{N_\mathrm{f}}{2g^2}\sigma^2, \tag{1}$$

where e is the elementary electric charge, N_f denotes the number of fermion flavors [the sum over flavors is implicit in (1)], and g^2 denotes the four-Fermi coupling constant. To arrive at Eq. (1), we have performed the usual Hubbard-Stratonovich transformation introducing the auxiliary scalar field σ in exchange for the $(\bar{\psi}\psi)^2$ term.

In this work, we consider a three-dimensional Euclidean space-time and work with four-component spinors, which allows for the definition of a matrix γ_5, anticommuting with all other gamma matrices. The model then has a $\mathbb{Z}_2$ chiral symmetry,[2] being invariant under the simultaneous transformations

$$\psi \to \gamma_5\psi, \qquad \bar{\psi} \to -\bar{\psi}\gamma_5, \qquad \sigma \to -\sigma. \tag{2}$$

This chiral symmetry may be spontaneously broken by the formation of a chiral condensate $\langle\bar{\psi}\psi\rangle$, which can be shown to be related to the expectation value of σ by means of a Dyson-Schwinger equation:

$$\langle\bar{\psi}\psi\rangle = \frac{\mathrm{i}N_\mathrm{f}}{g^2}\langle\sigma\rangle. \tag{3}$$

In [15] we presented a computation of the effective potential V_eff of the GN model in $2+1$ dimensions in the limit $N_\mathrm{f}\to\infty$, where the mean-field approximation becomes exact. Assuming translational invariance in space and time, $\sigma(x)=\sigma=\mathrm{const}$, and that the magnetic field lies perpendicular to the spatial plane and has a magnitude B such that, without loss of generality, $eB>0$, one finds (see also [28])

$$V_\mathrm{eff}(\sigma) = -\frac{\sigma^2}{2\pi}\sigma_0 - \frac{\sqrt{2}}{\pi}(eB)^{3/2}\zeta_H\left(-\frac{1}{2},\frac{\sigma^2}{2eB}\right) + \frac{|\sigma|eB}{2\pi} - \frac{eB}{2\pi\beta}\sum_{l=0}^{\infty} d_l\left[\ln\left(1+e^{-\beta(\sqrt{\sigma^2+2eBl}+\mu)}\right) + (\mu\leftrightarrow-\mu)\right], \tag{4}$$

where ζ_H denotes the Hurwitz zeta function and $\beta=1/T$ is the inverse temperature. The sum runs over the fermionic Landau levels, labeled by the index l, and $d_l=2-\delta_{l0}$ takes into account that the degeneracy of the lowest Landau level (LLL) is only half of that of the higher ones.

Because of (3), the chiral condensate in the large-N_f limit is proportional to the position of the global minimum of $V_\mathrm{eff}(\sigma)$, i.e., to the solution $\langle\sigma\rangle$ of the gap equation

$$V'_\mathrm{eff}(\sigma)|_{\sigma=\langle\sigma\rangle} = 0. \tag{5}$$

In the following, we denote by σ_0 the value of $\langle\sigma\rangle$ at zero temperature, chemical potential, and magnetic field. We are interested in the phase structure of the model at finite chemical potential and vanishing to low temperature. To this end, we have performed a minimization of V_eff in the (B,μ) plane, and we show the $T=0$ phase diagram in Fig. 1 (left).

A striking feature of the (B,μ) phase structure at zero temperature is the cascade of first-order[3] phase transitions in μ for small eB. The physical origin of these multiple phase transitions lies in the discreteness of Landau levels. As long as B is small, the Landau levels are closely spaced, such that for increasing chemical potential the Fermi energy crosses them successively, resulting in the possibility for the order parameter to jump discontinuously for every such crossing. When the magnetic field is strong enough, however, the

[1]For a recent update on the status of open science within the lattice community, see Ref. [25].

[2]Strictly speaking, there is no chiral symmetry in odd dimensions. Here, it refers to the symmetry in the reducible representation inherited from chiral symmetry in four dimensions.

[3]We remark that for $B=0$ the (single) phase transition is of second order everywhere but at the point $(T=0,\mu=\sigma_0)$, where it becomes degenerate.

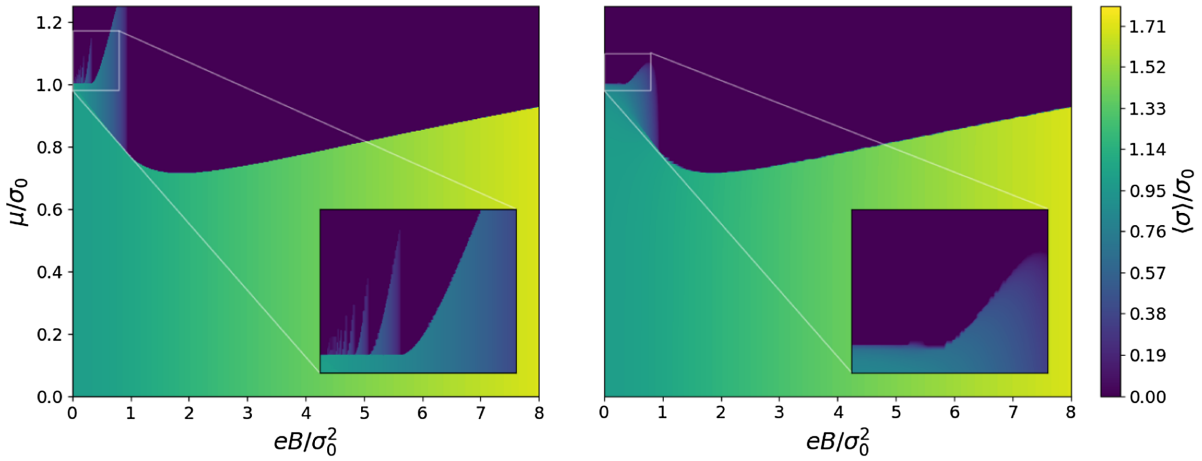

FIG. 1. (B, μ) phase diagram of the $(2+1)$-dimensional GN model in the mean-field limit at $T = 0$ (left) and $T = 0.1\sigma_0$ (right). The insets show enlarged regions where multiple phase transitions occur.

energy difference between Landau levels grows too large and only the LLL remains occupied, such that only the chiral phase transition (i.e., the transition from $\langle\sigma\rangle \neq 0$ to $\langle\sigma\rangle = 0$), but no intermediate transition, is seen.

As can be seen in Fig. 1 (right), thermal fluctuations present at $T \neq 0$ wash out the pattern of multiple phase transitions. This can be understood by recalling that at finite temperature the underlying Fermi-Dirac distribution is no longer a step function but becomes smoother, which, in turn, results in a smoother behavior of the order parameter as the Landau levels are crossed. Still, even at $T/\sigma_0 = 0.1$, an intermediate phase can be found for small eB and large μ. We also mention that the critical chemical potential μ_c of the chiral phase transition shows a nonmonotonic behavior in B as long as the latter is not too strong, while it grows monotonically for larger eB.

Moreover, one observes that generically the phase diagram is roughly divided into two regions: the large *magnetic catalysis* region, where the order parameter increases with the magnetic field, and the smaller *inverse magnetic catalysis* region, where it decreases with B. We emphasize the stark contrast to the situation at zero density studied in [15], where only magnetic catalysis is present for all magnetic field strengths and temperatures.

A physical explanation for magnetic catalysis is provided in [29] by the effective reduction of the number of space-time dimensions due to the presence of the magnetic field, which causes infrared divergences to which the system responds via the formation of a mass gap. The inverse magnetic catalysis found for weak magnetic fields and large chemical potentials, on the other hand, was explained in [30,31] to be caused by a competition between the energy gain due to the formation of a chiral condensate (which increases with B) and the energy cost of overcoming the imbalance between fermions and antifermions at finite μ (which increases with both B and μ).

Note that in the context of finite-temperature QCD the expression "inverse magnetic catalysis" commonly refers to the decrease of the chiral crossover temperature with B, accompanied by a nonmonotonic B dependence of the chiral condensate [16,17]. One should, however, be careful when comparing the situation in QCD to the one considered here, since their physical origins appear to be quite different.

Finally, we mention that the lattice study [32] provided evidence for the existence of a tricritical point in the (T, μ) plane at $B = 0$, accompanied by a first-order transition line for nonvanishing temperatures, in contradiction to the known mean-field results. While in analytical beyond-large-N_f studies such as the OPT calculations [33,34] a similar result was found, we argue that one may encounter first-order transitions at the mean-field level as well, provided that one studies the theory on a finite spatial volume. The reasoning is as follows: On a finite volume, the allowed momenta and, thus, the one-particle energies are discrete, which can give rise to discontinuous phase transitions in the same way as the Landau quantization. In a way, the $B = 0$ theory in a finite volume is thus reminiscent of the $B \neq 0$ theory.

More concretely, the GN effective potential for vanishing magnetic field on a finite spatial volume L^2, such that the space-time volume reads $V = \beta L^2$, is given by

$$V_{\mathrm{eff}}(\sigma)|_{B=0} = -\frac{\sigma^2}{2\pi}\sigma_0 + \frac{|\sigma|^3}{3\pi} + \frac{\sigma}{\pi L^2}{\sum_{\mathbf{n}}}' e^{-L\sigma|\mathbf{n}|}\frac{1}{\mathbf{n}^2}\left(1 + \frac{1}{L\sigma|\mathbf{n}|}\right) - \frac{2}{V}\sum_{\mathbf{p}}\left[\ln\left(1 + e^{-\beta(\sqrt{\sigma^2+\mathbf{p}^2}+\mu)}\right) + (\mu \leftrightarrow -\mu)\right], \tag{6}$$

where $\mathbf{n} = (n_1, n_2) \in \mathbb{Z}^2$ and the prime on the first sum indicates omission of the summand where $n_1 = n_2 = 0$, while the second sum runs over spatial momenta $\mathbf{p} = \frac{2\pi}{L}\mathbf{n}$. The derivation is similar as in the $B \neq 0$ case, with the sum over Landau levels being replaced by momentum sums; see, e.g., [35].

The first sum in (6) represents the finite-size corrections to V_{eff}, while the last term is the analog of the last term in (4) on a finite volume and for vanishing magnetic field, and thus—notice their similarity—may also give rise to discontinuities at low temperatures. We remark that σ_0 in (6) refers to the value of the condensate for vanishing B, T, and μ in the infinite-volume limit, as above, and not its finite-volume counterpart.

We show in Fig. 2 a comparison between the effective potential at the chiral phase transition for both finite and infinite L (always assumed equal in both directions) at a low nonvanishing temperature. We see that on the finite volumes V_{eff} exhibits three degenerate global minima: one at $\sigma = 0$ and two at nontrivial values of σ related to one another via a chiral transformation. The minima are separated by potential barriers, which is indicative of a first-order phase transition, since it implies the coexistence of two phases. For $L = \infty$, on the other hand, the nontrivial minima turn into the trivial one in a smooth way when increasing μ, which rather hints at a second-order transition. A more detailed analysis on finite-volume effects will be the subject of a forthcoming publication.

Since our lattice simulations are all performed on finite volumes, they could conceivably reveal a first-order transition as well, leading us to investigate this question in more detail below. We remark, however, that a weak nonvanishing magnetic field on finite volumes and at nonzero temperatures might, in fact, drive the system back to a second-order phase transition, which then becomes first order again only for strong enough B. Also, there are

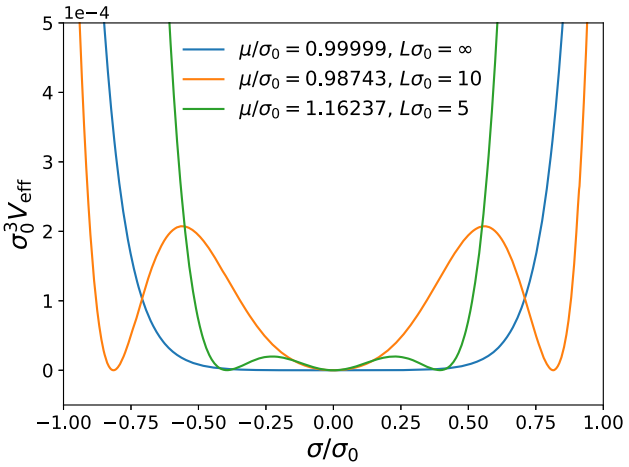

FIG. 2. V_{eff} as a function of σ for $T/\sigma_0 = 0.1$ at the chiral phase transition, $\mu = \mu_c(T)$, and for different L.

examples where first-order phase transitions found under the assumption of homogeneity were later understood to be of second order after lifting the latter constraint [36]. In [37], we developed the technology to investigate this on the lattice.

Finally, we emphasize the nonmonotonic behavior of the critical chemical potential with L in Fig. 2, which is reminiscent of the B dependence of μ_c for a sufficiently weak magnetic field. From these observations, one clearly realizes that the interplay between nonzero magnetic field, temperature, and chemical potential has a highly nontrivial influence on the order parameter even in the infinite-volume limit and becomes even more involved once $L < \infty$ enters as an additional control parameter. We also mention the possibility of introducing a tilt in the magnetic field, resulting in a nontrivial phase structure even at zero chemical potential [38,39].

III. NUMERICAL SETUP

A. Simulations with overlap fermions

We perform lattice simulations of the $(2+1)$-dimensional GN model using one reducible four-component flavor, $N_f = 1$, of Neuberger's overlap fermions [40]. We couple the chemical potential μ in a way suggested by Gavai and Sharma [41], such that our full lattice Dirac operator reads

$$D = (\sigma + \mu\gamma_0)\left(\mathbb{1} - \frac{a}{2}D_{\text{ov}}\right) + D_{\text{ov}}, \tag{7}$$

where D_{ov} is the massless overlap operator,

$$D_{\text{ov}} = \frac{1}{a}\left(\mathbb{1} + D_W(-1)\Big/\sqrt{D_W^\dagger(-1)D_W(-1)}\right), \tag{8}$$

a denotes the lattice constant, and $D_W(am)$ is the standard Wilson operator with mass m. D_W also contains the $U(1)$ link variables encoding the magnetic field. For more details on the discretization, including a thorough discussion on how the magnetic field is implemented in our simulations as well as a number of numerical tests, we refer to [15].

There, we also argue that the lattice chiral condensate [42] is related to the expectation value of σ via

$$\left\langle \bar{\psi}\left(\mathbb{1} - \frac{a}{2}D_{\text{ov}}\right)\psi \right\rangle = -\frac{N_f}{g^2}\langle\sigma\rangle, \tag{9}$$

in analogy to the continuum expression (3). As in [15], we use the observable $\langle|\bar{\sigma}|\rangle$, where $\bar{\sigma}$ denotes the space-time average of σ, as an order parameter for chiral symmetry breaking, and we perform the scale setting at $\mu = B = 0$ and at low temperatures. A detailed list of the parameter values used in our simulations can be found in Appendix B.

B. The complex-action problem

In [15], we showed that our lattice action is real for arbitrary B at vanishing μ and the same holds true in the case $B = 0$ and $\mu \neq 0$. In this work, we are, however, concerned with B and μ both being nonzero, such that we have to expect a complex-action problem in general. However, we found numerically that the ensuing complex-action problem is, in fact, mild—in particular, with respect to the estimation of the chiral condensate. The fluctuating phase then gives rise only to a systematic uncertainty, which we estimate on exemplary ensembles. Most importantly, we demonstrate in the following that it is negligible compared to the statistical uncertainties.

For the expectation value of an observable $\mathcal{O}$, the standard reweighting approach

$$\langle \mathcal{O} \rangle = \frac{\int \mathcal{D}\sigma e^{-S_R - \mathrm{i}S_I}\mathcal{O}}{\int \mathcal{D}\sigma e^{-S_R - \mathrm{i}S_I}} = \frac{\langle e^{-\mathrm{i}S_I}\mathcal{O}\rangle_R}{\langle e^{-\mathrm{i}S_I}\rangle_R} \tag{10}$$

provides an exact representation with stochastic interpretation in the presence of a complex action $S = S_R + \mathrm{i}S_I$ with $S_R, S_I \in \mathbb{R}$. Here, $\langle\cdot\rangle_R$ denotes the expectation value with respect to the probability distribution e^{-S_R}/Z_R for an appropriate normalization Z_R. As is well known, this expression does not solve the complex-action problem, because the numerical determination of the quotient on the right-hand side of (10), in general, requires an exponential amount of computational resources in the thermodynamic limit [43]. However, this statement is concerned with only the asymptotic behavior, and, depending on the observable in question, the desired parameter regime might still be reachable at a reasonable numerical cost.

More precisely, if the covariance between $\mathcal{O}$ and $e^{\mathrm{i}S_I}$ is negligible compared to the average phase $\langle e^{-\mathrm{i}S_I}\rangle_R$, the latter approximately drops out of the expectation value:

$$\langle \mathcal{O} \rangle = \langle \mathcal{O} \rangle_R + \frac{\mathrm{cov}_R(e^{-\mathrm{i}S_I}, \mathcal{O})}{\langle e^{-\mathrm{i}S_I}\rangle_R} \approx \langle \mathcal{O} \rangle_R, \tag{11}$$

where the covariance between two random variables X and Y is defined as

$$\mathrm{cov}_R(X, Y) = \langle (X - \langle X\rangle_R)(Y - \langle Y\rangle_R)\rangle_R. \tag{12}$$

In this work, we are predominantly concerned with the computation of the chiral condensate, $\mathcal{O} = |\bar{\sigma}|$. In Appendix A, we show exemplary data that we used to estimate the systematic uncertainties arising from the second term in (11). In summary, we found that

$$\mathrm{cov}_R(e^{-\mathrm{i}S_I}, |\bar{\sigma}|) \sim \mathcal{O}(10^{-4}\ldots 10^{-2}), \tag{13}$$

while

$$|1 - \langle e^{-\mathrm{i}S_I}\rangle_R| \sim \mathcal{O}(10^{-3}\ldots 10^{-1}), \tag{14}$$

such that overall we expect systematic uncertainties of $\mathcal{O}(10^{-3})$ from negligence of the complex-action problem, while our statistical uncertainties are typically of $\mathcal{O}(10^{-2})$. We conclude that we may safely neglect the complex-action problem on our small- and medium-sized lattices. Future research on larger lattices might have to review this position, however.

IV. RESULTS

In the following, we present our lattice results for the chiral condensate in the parameter space spanned by the chemical potential μ and the magnetic field B at a low temperature T. In particular, we aim at answering the question of what remains of the large-N_f phase structure shown in Figs. 1 and 2 when considering $N_\mathrm{f} = 1$. Hence, we look for traces of inverse magnetic catalysis, multiple phase transitions in μ at $B \neq 0$, and a first-order transition at $B = 0$. Throughout, N_s and N_t denote the number of lattice points in each spatial and the temporal direction, respectively. Moreover, we employ periodic boundary conditions in space and antiperiodic ones in time for fermions, while the scalar field σ is periodic in all directions.

We begin by showing in Fig. 3 an infinite-volume extrapolation at fixed lattice spacing of $\langle|\bar{\sigma}|\rangle(\mu)$ for various values of B. In what follows, we shall discuss these results in more detail.

A. Vanishing magnetic field

Focusing on $B = 0$ first, one observes that, as anticipated, chiral symmetry is spontaneously broken at $\mu = 0$, indicated by $\langle|\bar{\sigma}|\rangle \neq 0$, and that the order parameter decreases with increasing μ (to a nonzero value due to our definition of $\langle|\bar{\sigma}|\rangle$). This behavior becomes sharper on larger volumes, which is the expected behavior for a phase transition. In order to determine the order of this transition, it is instructive to study histograms of $\bar{\sigma}$, as they allow one to reproduce the probability distribution e^{-S_R}/Z_R. We show the effective potential determined from this distribution in the vicinity of the phase transition on our smallest lattice in Fig. 4. The corresponding temperature amounts to $T/\sigma_0 \approx 0.118$; i.e., it is significantly different from zero.

One observes that for $\mu/\sigma_0 \approx 0.282$ the potential has two degenerate minima at $\bar{\sigma}/\sigma_0 \approx \pm 1$, while for $\mu/\sigma_0 \approx 0.301$ a third minimum emerges at $\bar{\sigma} = 0$. Finally, at $\mu/\sigma_0 \approx 0.376$, only this trivial minimum is left. This is clear evidence for a first-order phase transition at $\mu = \mu_\mathrm{c} \approx 0.301\sigma_0$. That this is the case even on a lattice volume as small as 8^2 does not really come as a surprise in light of the discussion regarding Fig. 2 in Sec. II. We notice that the critical chemical potential μ_c is roughly 3 times smaller than in the large-N_f limit. This reduction is less than the factor of around 4 or 5 found for the zero-density critical temperature in [15].

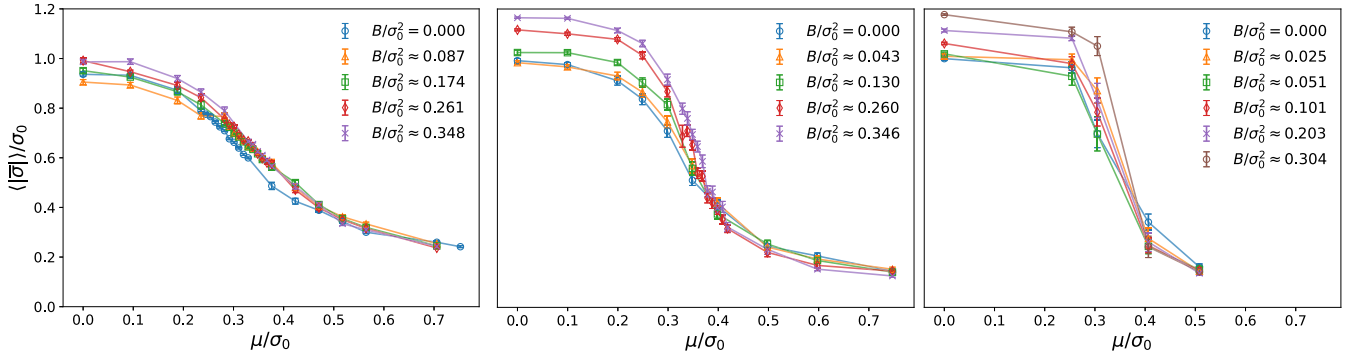

FIG. 3. Order parameter $\langle|\bar{\sigma}|\rangle$ as a function of μ for different magnetic field strengths in an infinite-volume extrapolation at fixed lattice spacing. (left) $N_s = 8$, $a\sigma_0 \approx 1.063$. (center) $N_s = 12$, $a\sigma_0 \approx 1.004$. (right) $N_s = 16$, $a\sigma_0 \approx 0.984$. We consider only cubic lattices where $N_s = N_t$.

We also remark that on small lattices the first-order transition is not visible from the μ dependence of $\langle|\bar{\sigma}|\rangle$ alone. However, as can be seen in Fig. 3, the transition becomes sharper for larger volumes and approaches the behavior one would expect from a first-order transition. This is due to the minima of S_{eff} deepening, making tunneling between them less probable. While a detailed analysis of the effective potential on our larger lattices was not possible due to limited statistics, we believe that the transition is of first order for all lattice sizes considered here.

Let us now compare our results at $B = 0$ with the existing literature. Previous works using staggered fermions at $N_f = 12$ [4] and $N_f = 4$ [32], respectively, report that the phase transition is of first order at $T \approx 0$ (simulations at exactly vanishing temperature are, of course, impossible) and of second order for relatively high temperatures. They also claim that their findings are consistent with the existence of a first-order critical line at low temperatures, ending in a tricritical point at some nonzero value of T, despite being unable to precisely locate this tricritical point. These results were also confirmed by the OPT studies [33,34].

Lastly, we mention that our estimate of μ_c, which is approximately $0.3\sigma_0$ for all lattice sizes considered, is significantly lower than the one quoted in [4], where it is comparable to the mean-field value, $\mu_c/\sigma_0 = 1$. However, this is expected, since quantum fluctuations tend to destroy long-range order and, thus, shrink the region of broken chiral symmetry.

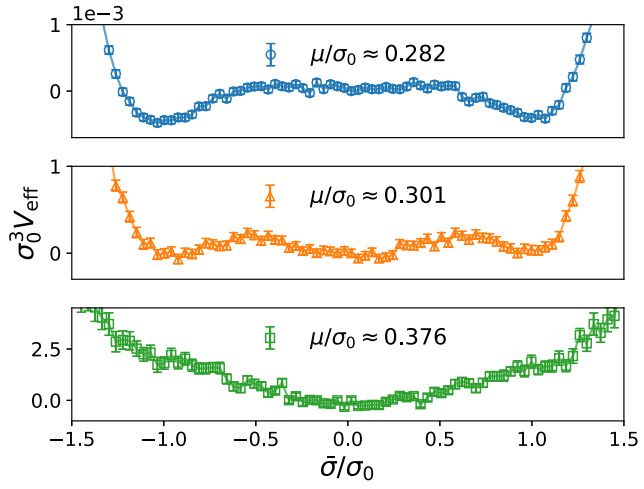

FIG. 4. Constraint effective potential [44] for $B = 0$, determined as the logarithm of the probability distribution of $\bar{\sigma}$ and normalized to zero at $\bar{\sigma} = 0$; $N_s = N_t = 8$ and $a\sigma_0 \approx 1.063$.

B. Finite magnetic field

Now turning to the case of $B \neq 0$, we see from Fig. 3 that for small μ the magnetic field has an overall tendency to increase the chiral condensate, corresponding to the magnetic catalysis scenario outlined in Sec. II. Notice, however, that on smaller lattices there are finite-volume effects that lead to a nonmonotonic B dependence of the chiral condensate: $\langle|\bar{\sigma}|\rangle$ first decreases for the weakest allowed nonvanishing magnetic field before increasing monotonically with B for all stronger fields. This effect was also observed in our previous study [15] and can even be seen at the mean-field level but ceases to play a role for larger volumes. While this nonmonotonicity could potentially be relevant for applications of the GN model in solid-state physics [45,46], we do not discuss it further here as our work rather takes its motivation from high-energy physics, where one typically assumes infinite volumes.

Investigating larger chemical potentials next, the situation appears very much unchanged in that—within the error margins—the magnetic field increases the order parameter for all μ below the phase transition apart from possible finite-size effects. The transition itself appears to remain a (weak) first-order one even for $B \neq 0$. Far beyond the phase transition, the magnetic field ceases to have a noticeable effect on $\langle|\bar{\sigma}|\rangle$, a behavior also observed in the finite-T

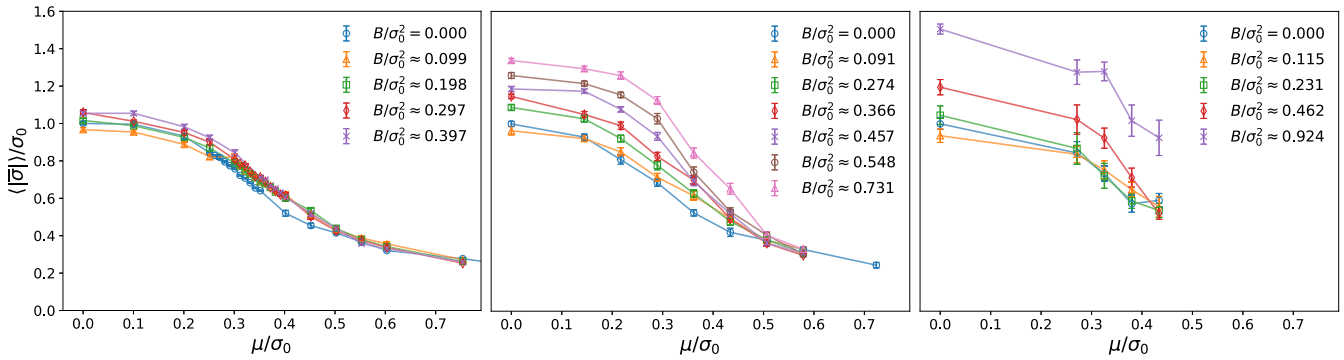

FIG. 5. Order parameter $\langle|\bar{\sigma}|\rangle$ as a function of μ for different magnetic field strengths in a continuum extrapolation at fixed physical volume. (left) $N_s = 8$, $a\sigma_0 \approx 0.995$. (center) $N_s = 12$, $a\sigma_0 \approx 0.691$. (right) $N_s = 16$, $a\sigma_0 \approx 0.461$. We consider only cubic lattices where $N_s = N_t$.

study [15]. We furthermore observe that the critical chemical potential of the transition slightly increases with B within errors.

These observations are in contradiction with the mean-field scenario of inverse magnetic catalysis discussed in Sec. II, as well as with the OPT study [19], where inverse magnetic catalysis was predicted to persist even beyond the large-N_f limit. Furthermore, we find no evidence for multiple phase transitions in μ at finite B, whereas they were claimed in [19] to exist even for $N_f = 2$. While the situation could, in principle, be qualitatively different between $N_f = 2$ and $N_f = 1$, we consider this rather unlikely and are inclined to look for alternative explanations for this discrepancy.[4]

It is important to stress that the missing features of inverse catalysis and cascades of phase transitions are expected to happen in a very small parameter region. In lack of a better guiding principle, one could assume that the reduction of the critical chemical potential as a scale roughly carries over to other features of the phase diagram. Even in the mean-field approximation, they occur only within $\pm 10 \ldots 20\%$ of the critical chemical potential—being themselves only a few percent; see Fig. 1. Scaling that down leads us to expect filigree features of the size of $\mu/\sigma_0 \sim \mathcal{O}(0.006)$ in a very small parameter regime of $\mathcal{O}(0.06)$—this is a scale that we cannot resolve with the current method assuming a reasonable amount of resources. Even stronger physical constraints on the sampling rate apply to the magnetic field's discretization due to the finite volume. As the multiple phase transitions quickly oscillate in that direction of the phase diagram, resolving, e.g., one of the spikes in the critical chemical potential seems quite unlikely.

[4]There are ongoing discussions about critical flavor numbers in related 2 + 1D Thirring models—see, e.g., [47–49]—but these are of a very different nature and we see no indication for similar phenomena to arise in this context.

Nevertheless, we would have expected at least some kind of footprint and the lack of any evidence begs an explanation. The main differences between [19] and the present work are that the former was performed in the continuum, in an infinite volume, and under the assumption that σ is homogeneous, while we consider the theory on a lattice of finite extent and allow for arbitrary modulations of σ. It is the latter difference, in particular, that could be responsible for the absence of multiple phase transitions, as strong fluctuations in σ could likely wash out the discrete Landau level structure, which is the origin of the cascade of transitions in the first place. While we investigate the potential existence of inhomogeneities in σ below, we mention that the precise reason for the absence of inverse magnetic catalysis and multiple phase transitions is still not entirely clear to us. Additional work in that direction, however, is ongoing and intended to be part of a forthcoming publication. It might also be enlightening to investigate whether the OPT's prediction is stable with respect to the inclusion of higher orders in $1/N_f$ given the very small flavor numbers we are discussing here.

In order to study stronger magnetic fields (in units of σ_0), we also approach the continuum limit for fixed physical volume and show the results for the μ dependence of the order parameter in Fig. 5. The observations are, however, in close analogy to the infinite-volume extrapolation discussed above: We find magnetic catalysis below the phase transition, a slight increase of μ_c with B, and no evidence for multiple phase transitions.

C. Inhomogeneous phases

Lastly, as in [15], we study the possibility of spatial inhomogeneities in σ induced by the magnetic field. While the zero-density study [15] did not observe any evidence of such inhomogeneous structures, this is hardly surprising as even in the (four-dimensional) mean-field calculations [21–23] inhomogeneities would arise only at $\mu \neq 0$. Conceptionally speaking, the magnetic field is capable

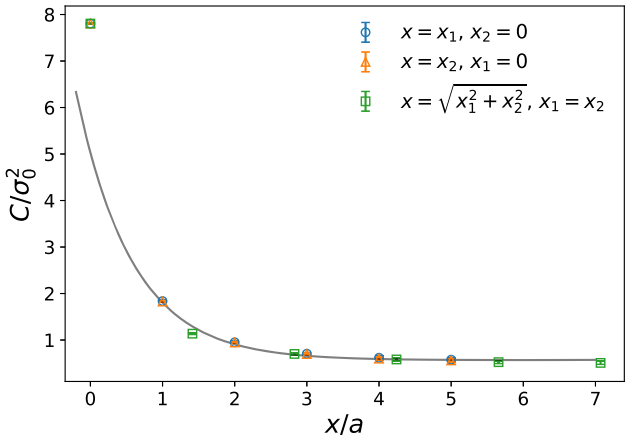

FIG. 6. Spatial correlator C from (15) along the coordinate axes (either $x_1 = 0$ or $x_2 = 0$) as well as the diagonal ($x_1 = x_2$) for $N_s = N_t = 12$, $eB/\sigma_0^2 \approx 0.346$, $\mu/\sigma_0 \approx 0.349$, and $a\sigma_0 \approx 1.004$. The full line corresponds to a cosh fit to the data points, starting from $x \geq a$, and is included in order to guide the eye and showcase rotational invariance.

of inducing inhomogeneities due to the effective reduction of the number of space-time dimensions for strong enough B. This is because in low dimensions four-Fermi theories (at $B = 0$) are known to develop inhomogeneous structures at finite density and low temperatures, as was first found in mean-field studies [36,50] and has recently been confirmed by lattice simulations at finite N_f [37,51,52].

In order to address this question, we follow [15,37] in computing the spatial correlation function

$$C(x_1, x_2) = \frac{1}{N_s^2 N_t} \sum_{x'} \langle \sigma(x_0', x_1, x_2) \sigma(x_0', x_1 + x_1', x_2 + x_2') \rangle, \tag{15}$$

where the x_i denote the spatial components of a lattice point and the sum over x' runs over the entire lattice. Any spatial inhomogeneities present in σ should also be visible in C, but the latter has the advantage that it does not suffer from cancellations as the expectation value of σ itself would [37]. However, as can be seen exemplarily in Fig. 6 for a relatively strong magnetic field at a low temperature and a chemical potential close to the phase transition, we do not find any evidence for inhomogeneities even in our simulations at $\mu \neq 0$. We have verified that the same is true for all of our other data points as well. We remark that earlier simulations of the model at vanishing magnetic field, using staggered fermions on larger lattices, did find signs of inhomogeneities [53].

V. DISCUSSION

In this work, we have presented the results of extensive lattice simulations of the Gross-Neveu model (1) in $2+1$ dimensions at finite chemical potential and magnetic field, considering $N_f = 1$ flavor of four-component overlap fermions. We argue that the arising complex-action problem is under control. The $\mu \neq 0$ simulations at $T \approx 0$ discussed here complement our previous results [15] obtained at $\mu = 0$ and $T \neq 0$.

It was the main goal of [15] and the present work to understand to what extent the rich phase structure in (B, T, μ) space the model exhibits in the mean-field limit ($N_f \to \infty$) persists when considering a finite flavor number. While at $\mu = 0$ the generic features of the large-N_f model, i.e., magnetic catalysis for all temperatures below the phase transition and an increase of the critical temperature with B, were found to be exist also for $N_f = 1$ [15], the situation at $\mu \neq 0$ appears to be different. There, the mean-field approximation predicts a cascade of first-order phase transitions and a region of inverse magnetic catalysis, i.e., a decrease of the order parameter with B. However, we find no evidence of either of these effects in our simulations. On the contrary, we find magnetic catalysis below and in the vicinity of the phase transition and an increase of the critical chemical potential with B. While—to the best of our knowledge—no previous lattice results exist addressing this question, our findings are in contradiction with analytical results using the OPT method to study the two-flavor theory, where the aforementioned features were found to persist [19].

We have already mentioned the most substantial differences between [19] and the present work in that the former works in the continuum, in an infinite volume, and assumes translational invariance, $\sigma(x) = \sigma$, while we work on a lattice of finite extent and allow for σ to vary in space and time. We believe that the latter difference could be responsible for the discrepancy, even though we find no trace of inhomogeneities at the level of Monte Carlo averages. Still, random fluctuations in σ could conceivably be strong enough to completely smear out the discretized energy levels induced by the Landau quantization causing the multiple-transition pattern. Moreover, the argument explaining the origin of inverse magnetic catalysis in [31] was also given under the assumption that the order parameter is constant, which could potentially invalidate it in the context of our lattice studies.

Another, perhaps less interesting, explanation is that the OPT method might plainly be not reliable for such small flavor numbers anymore. A follow-up study dealing with this discrepancy with more rigor, also considering larger N_f, is currently ongoing. We mention in passing that our simulations were performed within the strong-coupling regime, where there is spontaneous symmetry breaking for $T = 0$ and $\mu = 0$ even at vanishing magnetic field. However, our observation that inverse magnetic catalysis and the cascade of phase transitions are both absent rather resembles the situation in the weak-coupling regime, where chiral symmetry is intact when T, μ, and B all vanish and is broken only for nonzero magnetic field [19].

We found that the phase transition in μ for all magnetic field strengths likely is of weak first order even at relatively high temperatures, $T/\sigma_0 \approx 0.1$, which in the mean-field limit happens only for nonvanishing B. Our results are, however, in agreement with the previous $B = 0$ lattice [4,32] and OPT [33,34] studies, the latter of which claim that this first-order phase transition is a consequence of $1/N_f$ corrections. However, we argue that on a finite volume a first-order transition at $B = 0$ and $T \neq 0$ can emerge in the large-N_f limit as well.

Lastly, we briefly comment on the potential relevance of our results for QCD. The results of [15], predicting magnetic catalysis for every temperature below the phase transition, are in disagreement with the inverse magnetic catalysis scenario taking place around the chiral crossover in QCD [16,17]. This discrepancy can be understood by the fact that around the crossover the "sea quark" contribution, encoding the backreaction of the (charged) quarks onto the (neutral) gluonic distribution, dominates over the "valence quark" contribution, which causes an enhancement of chiral symmetry breaking [54]. This dominance of the sea quark effect then causes the chiral condensate to decrease. On the other hand, the purely fermionic GN model is, without modifications (see, e.g., [55–57]), obviously incapable of reproducing this gluon-induced phenomenology.

For temperatures far above and below the QCD crossover, however, the valence contribution dominates. If this were true at finite density as well, one could speculate that gluonic effects might be less relevant for the low-temperature regime at finite chemical potential we studied in this work. This would imply that our results might be of relevance for the finite-density regime of QCD, at least on a qualitative level. However, further research in that direction is certainly necessary in order to make any definite statements, since our $(2 + 1)$-dimensional model at $N_f = 1$ is clearly still quite different from QCD.

Full data underlying this work are available at Ref. [24]. Fully automated analysis work flows can be found at Ref. [27]. Raw data and the simulation code for generating the configurations are available upon request.

ACKNOWLEDGMENTS

This work would not have been possible without the simulation framework provided by Björn Wellegehausen. M. M. is indebted to Laurin Pannullo, Malte Schulze, Ivan Soler, and Marc Winstel for useful discussions. J. J. L. thanks Ed Bennett for helpful discussions about the reproducibility and openness of this publication. This work has been funded by the Deutsche Forschungsgemeinschaft (DFG) under Grant No. 406116891 within the Research Training Group RTG 2522/1. The work of J. J. L. was supported by the UKRI Science and Technology Facilities Council (STFC) Research Software Engineering Fellowship EP/V052489/1 and by the Supercomputing Wales project, which is part funded by the European Regional Development Fund (ERDF) via Welsh Government. The simulations were performed on resources of the Friedrich Schiller University in Jena supported in part by the DFG Grants No. INST 275/334-1 FUGG and No. INST 275/363-1 FUGG, as well as on the Swansea University SUNBIRD cluster (part of the Supercomputing Wales project). The Swansea University SUNBIRD system is part funded by the European Regional Development Fund (ERDF) via Welsh Government.

APPENDIX A: COMPLEX-ACTION PROBLEM

In the main text, we hinted that, while there is a non-negligible complex-action problem of up to 10%, the complex phase of the action is almost uncorrelated with the chiral condensate $\langle|\bar{\sigma}|\rangle$, the observable of predominant interest in this paper. In this scenario, it would be justifiable to neglect the complex-action problem for estimation of this particular observable, and we shall establish in this appendix that this is indeed the case.

Because of the significant computational cost, we have estimated the complex phase for a given ensemble only on a randomly drawn subset of configurations. We have always made sure that the number of randomly drawn configurations is significantly smaller than the effective number of statistically independent configurations while being large enough for reliable statistical estimates. For details of this procedure, we refer the reader to the corresponding code publication [27]. In the following, all analysis is done with respect to such subensembles.

Figure 7 shows the average phase and the covariance (12) between $|\bar{\sigma}|$ and the complex phase of the action. The four panels show different lattices. Because of the excessive

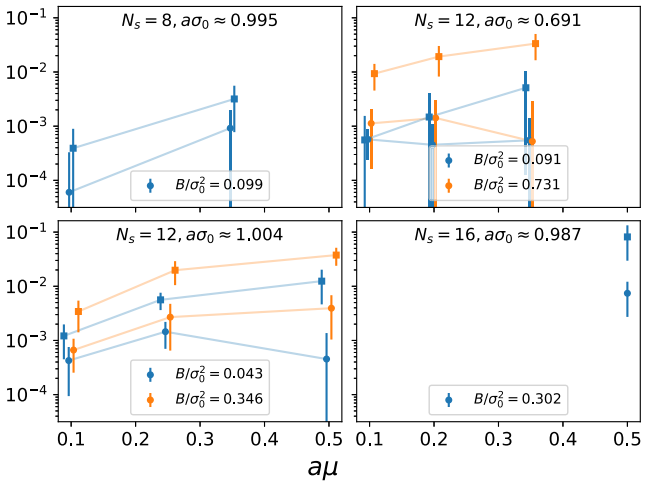

FIG. 7. Average phase (squares) and covariance between chiral condensate and complex phase of the action (circles) for different lattices over the chemical potential. Points are horizontally shifted for better visibility.

numerical cost, we could provide only a single data point for $N_s = 16$ for consistency checks. One should note that we have taken the absolute value here in order to capture the maximal possible effect in a single (real) number. Both quantities are complex valued, in general.

The data show the expected trend: The average phase becomes smaller (i.e., the complex-action problem becomes more severe) with growing μ and/or B. The maximal deviation of the average phase from unity is roughly 0.1 for the largest μ and B considered.

The covariance consistently is about an order of magnitude smaller on average and often even compatible with 0. One could conjecture that there is an analytical argument for the independence of the average phase and $\langle|\bar{\sigma}|\rangle$, but we have not found one yet. Moreover, the errors of both quantities are well under control, although the sample size for $N_s = 16$ is very small due to the excessive cost of computing the full determinant.

APPENDIX B: PARAMETERS

In Table I, we list the parameters used in our simulations. The magnetic flux quantum number b appears in the quantization condition of the magnetic field on the lattice:

$$eB = \frac{2\pi}{L^2} b, \tag{B1}$$

with L^2 denoting the area of the spatial plane. For further details on the simulations and the way we perform our error analysis, we refer to [15].

TABLE I. Parameters we have generated configurations for. N_s (N_t) denotes the number of lattice points in spatial (temporal) direction, g^2 is the four-Fermi coupling in Eq. (1), b denotes the magnetic flux quantum number in Eq. (B1), $a\mu$ is the chemical potential in lattice units, and T_0 denotes the temperature at which we set the scale σ_0, which we give in lattice units in the last column. Notice that T_0 differs between the infinite-volume and continuum extrapolations; see Ref. [15].

N_s	N_t	$1/g^2$	b	$a\mu$	T_0/σ_0	$a\sigma_0$
Infinite-volume extrapolation						
8	8	0.1520	0, 1, 2, 3, 4 0 1, 2 3 4	0.00, 0.10, 0.20, 0.25,…, 0.60, 0.75 0.26, 0.27,…, 0.34 0.31, 0.32,…, 0.38 0.31, 0.32,…, 0.39 0.36, 0.37, 0.38, 0.39	0.059	1.063
8	16	0.1520	0	0	0.059	1.063
12	12	0.1520	0, 1, 2, 3, 4, 6, 8 0, 1, 3, 6, 8 6, 8	0.00 0.10, 0.20, 0.25, …, 0.40, 0.50, 0.60, 0.75 0.33, 0.34, …, 0.42	0.062	1.004
12	16	0.1520	0	0	0.062	1.004
16	16	0.1520	0, 1, 2, 4, 8, 12, 16 0, 1, 2, 4, 8, 12	0.00 0.25, 0.30, 0.40, 0.50	0.064	0.984
Continuum extrapolation						
8	8	0.1520		(see above)	0.126	0.995
12	12	0.1650	0 1, 3, 4, 5, 6, 8 2	0.00, 0.10, 0.15, …, 0.40, 0.50 0.00, 0.10, 0.15, …, 0.40 0.00	0.121	0.691
16	16	0.1740	0, 1, 2, 3, 4, 6, 8, 12, 14, 16 0, 1, 2, 4, 8	0.00 0.125, 0.150, 0.175, 0.200	0.136	0.461

[1] M. Troyer and U.-J. Wiese, Phys. Rev. Lett. **94**, 170201 (2005).
[2] S. Scherer, Adv. Nucl. Phys. **27**, 277 (2003).
[3] K.-I. Kondo, Phys. Rev. D **82**, 065024 (2010).
[4] S. J. Hands, A. Kocić, and J. B. Kogut, Nucl. Phys. **B390**, 355 (1993).
[5] U. Vogl and W. Weise, Prog. Part. Nucl. Phys. **27**, 195 (1991).
[6] S. P. Klevansky, Rev. Mod. Phys. **64**, 649 (1992).

[7] C. G. Strouthos, Eur. Phys. J. A **18**, 211 (2003).
[8] I. A. Shovkovy, Lect. Notes Phys. **871**, 13 (2013).
[9] V. A. Miransky and I. A. Shovkovy, Phys. Rep. **576**, 1 (2015).
[10] J. O. Andersen, W. R. Naylor, and A. Tranberg, Rev. Mod. Phys. **88**, 025001 (2016).
[11] K. Tuchin, Adv. High Energy Phys. **2013**, 490495 (2013).
[12] E. J. Ferrer, V. de la Incera, J. P. Keith, I. Portillo, and P. L. Springsteen, Phys. Rev. C **82**, 065802 (2010).
[13] T. Vachaspati, Phys. Lett. B **265**, 258 (1991).
[14] D. J. Gross and A. Neveu, Phys. Rev. D **10**, 3235 (1974).
[15] J. J. Lenz, M. Mandl, and A. Wipf, Phys. Rev. D **107**, 094505 (2023).
[16] G. S. Bali, F. Bruckmann, G. Endrődi, Z. Fodor, S. D. Katz, S. Krieg, A. Schäfer, and K. K. Szabó, J. High Energy Phys. 02 (2012) 044.
[17] G. S. Bali, F. Bruckmann, G. Endrődi, Z. Fodor, S. D. Katz, and A. Schäfer, Phys. Rev. D **86**, 071502(R) (2012).
[18] A. S. Vshivtsev, K. G. Klimenko, and B. V. Magnitsky, Theor. Math. Phys. **106**, 319 (1996).
[19] J.-L. Kneur, M. B. Pinto, and R. O. Ramos, Phys. Rev. D **88**, 045005 (2013).
[20] G. Başar, G. V. Dunne, and D. E. Kharzeev, Phys. Rev. Lett. **104**, 232301 (2010).
[21] I. E. Frolov, V. Ch. Zhukovsky, and K. G. Klimenko, Phys. Rev. D **82**, 076002 (2010).
[22] T. Tatsumi, K. Nishiyama, and S. Karasawa, Phys. Lett. B **743**, 66 (2015).
[23] M. Buballa and S. Carignano, Eur. Phys. J. A **52**, 57 (2016).
[24] J. J. Lenz, M. Mandl, and A. Wipf, Dataset for "The magnetized $(2+1)$-dimensional Gross-Neveu model at finite density", 10.5281/zenodo.8201661.
[25] A. Athenodorou, E. Bennett, J. Lenz, and E. Papadopoullou, Proc. Sci. LATTICE2022 (**2023**) 341 [arXiv:2212.04853].
[26] M. D. Wilkinson *et al.*, Sci. Data **3**, 160018 (2016).
[27] J. J. Lenz, M. Mandl, and A. Wipf, Analysis and visualisation code for "The magnetized $(2+1)$-dimensional Gross-Neveu model at finite density", 10.5281/zenodo.8201673.
[28] V. P. Gusynin, V. A. Miransky, and I. A. Shovkovy, Phys. Rev. D **52**, 4718 (1995).
[29] V. P. Gusynin, V. A. Miransky, and I. A. Shovkovy, Phys. Rev. Lett. **73**, 3499 (1994); **76**, 1005(E) (1996).
[30] F. Preis, A. Rebhan, and A. Schmitt, J. High Energy Phys. 03 (2011) 033.
[31] F. Preis, A. Rebhan, and A. Schmitt, Lect. Notes Phys. **871**, 51 (2013).
[32] J. B. Kogut and C. G. Strouthos, Phys. Rev. D **63**, 054502 (2001).
[33] J.-L. Kneur, M. B. Pinto, R. O. Ramos, and E. Staudt, Phys. Rev. D **76**, 045020 (2007).
[34] J.-L. Kneur, M. B. Pinto, R. O. Ramos, and E. Staudt, Phys. Lett. B **657**, 136 (2007).
[35] A. Wipf, *Statistical Approach to Quantum Field Theory: An Introduction*, Lecture Notes in Physics Vol. 992 (Springer, New York, 2021), 10.1007/978-3-030-83263-6.
[36] M. Thies and K. Urlichs, Phys. Rev. D **67**, 125015 (2003).
[37] J. Lenz, L. Pannullo, M. Wagner, B. Wellegehausen, and A. Wipf, Phys. Rev. D **101**, 094512 (2020).
[38] K. G. Klimenko and R. N. Zhokhov, Phys. Rev. D **88**, 105015 (2013).
[39] R. N. Zhokhov, P. B. Kolmakov, V. C. Zhukovsky, and K. G. Klimenko, EPJ Web Conf. **126**, 04057 (2016).
[40] H. Neuberger, Phys. Lett. B **417**, 141 (1998).
[41] R. V. Gavai and S. Sharma, Phys. Lett. B **716**, 446 (2012).
[42] S. Chandrasekharan, Phys. Rev. D **60**, 074503 (1999).
[43] C. Gattringer and K. Langfeld, Int. J. Mod. Phys. A **31**, 1643007 (2016).
[44] L. O'Raifeartaigh, A. Wipf, and H. Yoneyama, Nucl. Phys. **B271**, 653 (1986).
[45] W. V. Liu, Nucl. Phys. **B556**, 563 (1999).
[46] I. F. Herbut and B. Roy, Phys. Rev. B **77**, 245438 (2008).
[47] J. J. Lenz, B. H. Wellegehausen, and A. Wipf, Phys. Rev. D **100**, 054501 (2019).
[48] A. W. Wipf and J. J. Lenz, Symmetry **14**, 333 (2022).
[49] S. Hands, Phys. Rev. D **99**, 034504 (2019).
[50] V. Schön and M. Thies, Phys. Rev. D **62**, 096002 (2000).
[51] J. J. Lenz, L. Pannullo, M. Wagner, B. H. Wellegehausen, and A. Wipf, Phys. Rev. D **102**, 114501 (2020).
[52] J. J. Lenz, M. Mandl, and A. Wipf, Phys. Rev. D **105**, 034512 (2022).
[53] S. Hands, J. B. Kogut, C. G. Strouthos, and T. N. Tran, Phys. Rev. D **68**, 016005 (2003).
[54] F. Bruckmann, G. Endrődi, and T. G. Kovács, J. High Energy Phys. 04 (2013) 112.
[55] A. Ayala, L. A. Hernández, M. Loewe, and C. Villavicencio, Eur. Phys. J. A **57**, 234 (2021).
[56] J. O. Andersen, Eur. Phys. J. A **57**, 189 (2021).
[57] A. Bandyopadhyay and R. L. S. Farias, Eur. Phys. J. Spec. Top. **230**, 719 (2021).